

Polarized Confocal Raman Microspectroscopy Studies of Chain Orientation on Injected Poly(propylene)/Montmorillonite Nanocomposites

D. García-López,¹ J. C. Merino,^{1,2} I. Gobernado-Mitre,¹ J. M. Pastor^{1,2}

¹CIDAUT, Centre for Automotive Research and Development, Parque Tecnológico de Boecillo, Parcela 209, ES-47151 Boecillo (Valladolid), Spain

²Departamento Física de la Materia Condensada, E.I.S.I.I., Universidad de Valladolid, 47011 Valladolid, Spain

Received 9 June 2004; accepted 20 September 2004

DOI 10.1002/app.21687

Published online in Wiley InterScience (www.interscience.wiley.com).

ABSTRACT: Molecular orientation along the depth of poly(propylene) (PP) and PP nanocomposite samples was analyzed by using confocal Raman microspectroscopy. The injection process led to a chain orientation that is higher on the surface of the samples. Residual stresses were relaxed through an annealing treatment, resulting in an increase of

the molecular orientation along the injection direction.
© 2005 Wiley Periodicals, Inc. *J Appl Polym Sci* 96: 2377–2382, 2005

Key words: nanocomposites; poly(propylene) (PP); Raman spectroscopy; injection molding; molecular orientation

INTRODUCTION

Nanocomposites constitute an emerging area of research and continue to be the focus of increasing attention. This new class of polymeric materials consists of a polymeric matrix with dispersed nanometer-scale particles. Different nanoparticles such as precipitated silica,¹ cellulose whiskers,² or carbon nanotubes, with three or two dimensions in the nanometric scale, have been reported. In this work, polymer nanocomposites based on layered silicates, which have a characteristic platelet shape and only one nanolevel dimension, were obtained and studied.

Polymer–clay nanocomposites have been widely studied in recent years. To achieve a good interaction between the inorganic material and the polymeric matrix, intercalation of organic compounds into the clay layers is needed. This leads to an expanded and organophilic layered structure. The organophilic clay is then incorporated into the polymer matrix by *in situ* polymerization or melt intercalation. When a good dispersion of the clay in the polymer matrix is achieved, significant improvements in mechanical^{3,4} and barrier properties,^{5,6} thermal stability,⁷ and flame retardance^{8,9} at low filler content (5 wt %) are observed. Therefore, these new materials may satisfy the ever-demanding requirements of materials for high-

technology applications. Furthermore, traditional processing technologies, such as extrusion or injection molding, may be used.

Montmorillonite (MMT), which is obtained from bentonite, is one of the most commonly used clays for the preparation of nanocomposites because of its high aspect ratio (500–1000) and a large surface area (750 m²/g). MMT exhibits a crystalline structure described by two-dimensional layers, which are composed of two tetrahedral sheets of silica surrounding an octahedral sheet of alumina or magnesia. Organic modification of the layered silicates is required to make them compatible with the polymer. The first compatibilizing agents used in the synthesis of polyamide-6–clay hybrids were amino acids.¹⁰ Numerous other kinds of compatibilizing agents have since been used, the most popular of which are alkylammonium ions because they can be easily exchanged with the Na⁺ or Ca²⁺ ions, thereby placing organic ions in the galleries between the silicate layers. Moreover, because of the nonpolar nature of the alkyl chain, they reduce the electrostatic interactions between the silicate layers, thus facilitating diffusion of the polymer into the galleries.

Despite the modification of the clay, achieving an exfoliated and homogeneous dispersion of the silicate layers at the nanometer level in nonpolar polymers, such as poly(propylene) (PP), is very difficult because of the high hydrophobicity of these polymers.¹¹ Consequently, the use of grafted PP with polar groups is necessary to achieve nanometric dispersion of the clay.^{12,13}

Correspondence to: J. Pastor (jmpastor@fmc.uva.es).

Contract grant sponsor: CICYT; contract grant number: MAT2002-04567-C02.

TABLE I
Composition of PP–MMT Nanocomposites

Sample	PP (wt %)	PP _g (wt %)	Clay	Modified agent	Clay (wt %)	TGA clay contents (wt %)
PP–MMT	86	7	MMT-I30.TC	ODA	7	4.5

It is well known that the mechanical and optical properties of injection-molded parts are strongly affected by molecular orientation. It may be expected that the orientation of PP chains along the injection direction will be influenced by the presence of the silicate layers. The purpose of this work was to examine the effect of injection molding on the surface and bulk molecular orientation in PP and PP–MMT nanocomposites using confocal Raman microspectroscopy. This technique offers a unique combination of spatial resolution and chemical/physical characterization.

EXPERIMENTAL

Materials

Isotactic polypropylene (Stamylan 17M10, from DSM N.V., Geleen, The Netherlands), maleic anhydride (MAH), grafted PP oligomer (Polybond 3200) with 1.2

wt % of MAH from Uniroyal Chemical (Middlebury, CT), and an organophilic montmorillonite (I30.TC) from Nanacor (West Lebanon, NH) were used for the preparation of poly(propylene) nanocomposites.

Preparation of nanocomposites

The first step was the preparation of a masterbatch by mixing the compatibilizing agent MAH and the clays in a Leistritz 27 GL intermeshing twin-screw extruder (Leistritz Extruder Corp, Somerville, NJ) with the temperature zones ranged from operating at 190 to 210°C and 50 rpm in a corrotating mode. The clay was added through a side feeder. Subsequently, the desired amounts of neat PP and the masterbatch were mixed in the twin-screw extruder at 190–210°C and 250 rpm. The composition of nanocomposites is detailed in Table I.

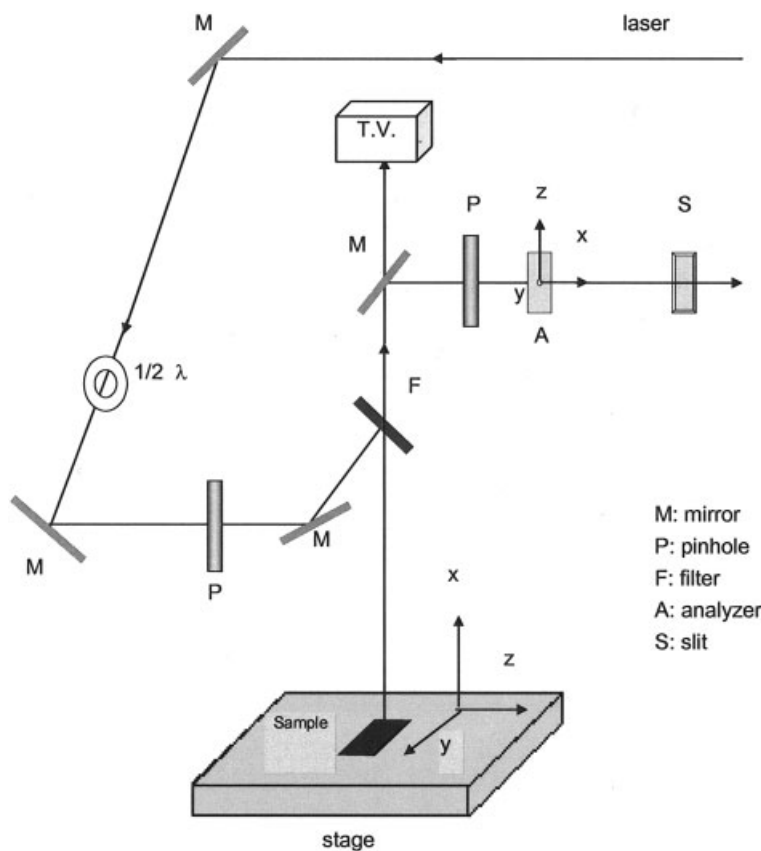
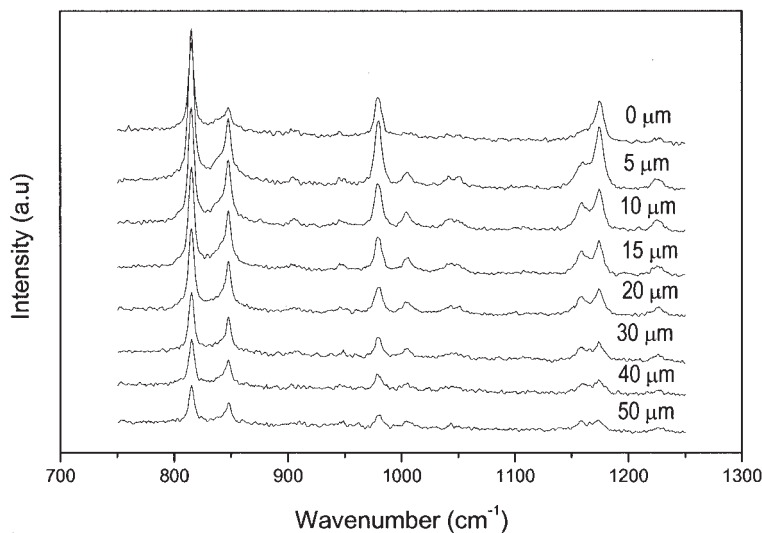
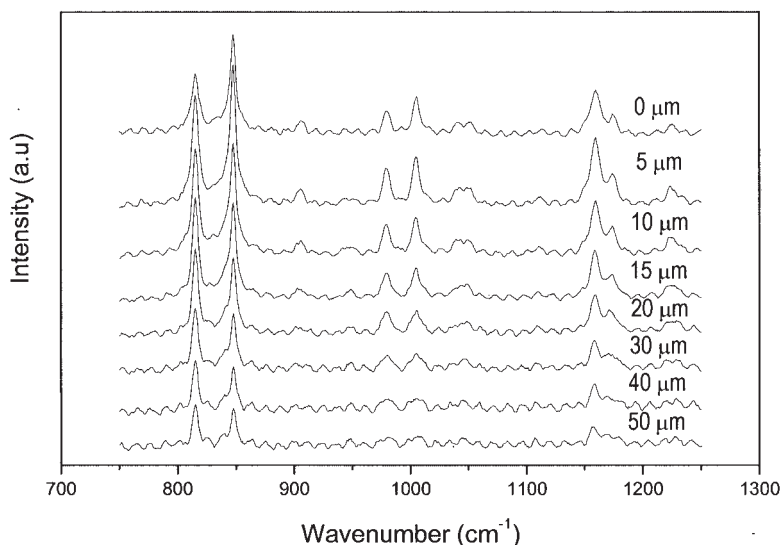


Figure 1 Optical system used for the polarized Raman microspectroscopy measurements.



(a)



(b)

Figure 2 Polarized Raman spectra in the spectral range of 800–1200 cm^{-1} for PP–MMT: (a) X(ZZ)X polarization; (b) X(YY)X polarization.

Dumbbell-shape test samples were obtained by injection molding using a Margarit JSW10 injection machine (Barcelona, Spain). The temperature of the cylinders was 190–200°C and the mold was kept at 40°C. Some injection-molded samples were annealed at 160°C for 2 h.

The clay content in the nanocomposites was measured by thermogravimetry analysis (TGA) using a TGA Model 851 furnace (Mettler Toledo International, Zurich, Switzerland) in an inert atmosphere, and 5 wt % of clay was obtained.

Confocal micro-Raman experiments

By coupling an optical microscope to a conventional Raman spectrometer under optimum conditions, lat-

eral and depth resolutions can be substantially enhanced.¹⁴ Micro-Raman spectra were measured on a LabRam microspectrometer (DILOR, Lyon, France) using a He–Ne laser beam operating at 632.8 nm, which supplies about 16 mW at the sample surface. The entrance slit was set to 500 μm , corresponding to spectral resolution of 4 cm^{-1} . Both the incident light and Raman scattering were collected through an Olympus (Tokyo, Japan) BH microscope with a 100 \times objective [numerical aperture (NA) = 0.90]. The confocal system contains a variable diaphragm (pin-hole) placed at the image plane of the microscope. This arrangement ensures that only light coming from upper and lower planes is partially attenuated. Thus, the

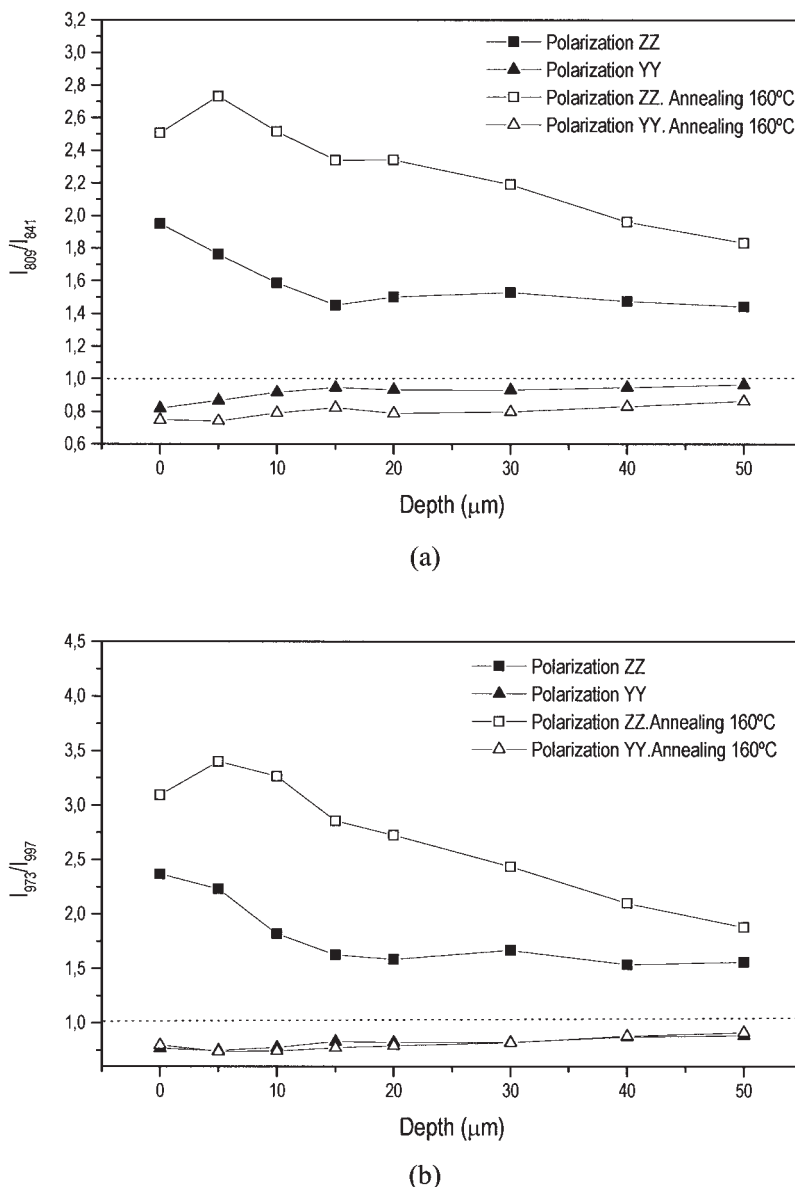


Figure 3 Raman intensity ratios versus distance from the surface of the PP sample: (a) I_{809}/I_{841} ; (b) I_{973}/I_{997} .

depth resolution of the microscope is also increased. The confocal microscope also offers improved lateral resolution compared with that of conventional microscopes. The combination of a $100\times$ objective with a pinhole of $100\text{-}\mu\text{m}$ diameter gives rise to a lateral resolution of about $1\text{ }\mu\text{m}$ and a depth resolution of about $2\text{ }\mu\text{m}$. The scanning time was 60 s and ten spectra were accumulated. The scattered light was detected with a CCD camera.

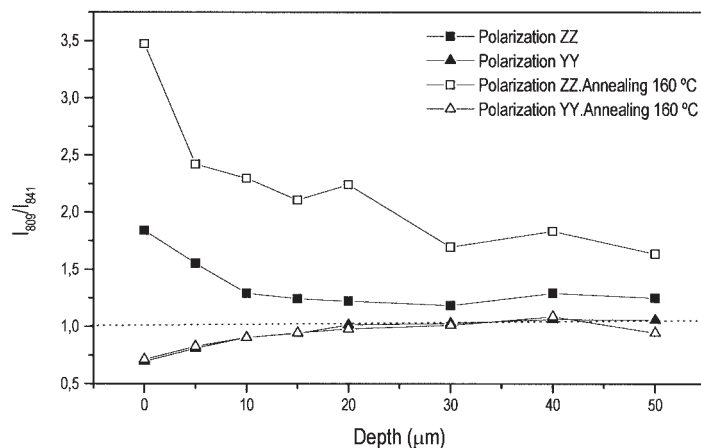
To analyze the influence of the injection process on the molecular orientation in the samples, an incident linearly polarized laser beam, in conjunction with a polarization analyzer for the collected Raman scattering, was used. In the polarizing optical system shown in Figure 1, the laser radiation is directed along the x -axis with its electric vector oriented along the y - or

z -axis. Using a half-wave plate, rotation of the plane of polarization of the incident laser beam was achieved. The analyzer was placed just in front of the spectrograph slit. Two different polarization geometries of the Raman experiment, represented according to Porto notation,¹⁵ were used: X(YY)X and X(ZZ)X (parallel/parallel condition).

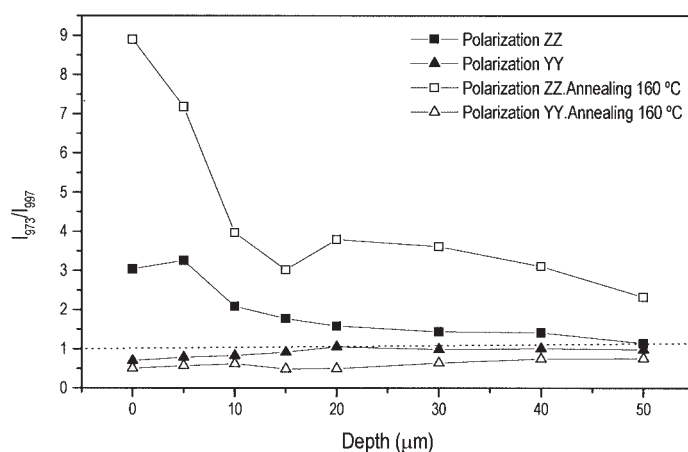
For the molecular characterization using Raman spectroscopy, no specific sample preparation was necessary.

RESULTS AND DISCUSSION

The Raman spectra were registered by focusing the laser beam beneath the surface on the center of the sample, with the incident laser and scattered light



(a)



(b)

Figure 4 Raman intensity ratios versus distance from the surface of the PP–MMT sample: (a) I_{809}/I_{841} ; (b) I_{973}/I_{997} .

polarized in a parallel or perpendicular direction with respect to the injection direction. The Raman bands detected at 809 and 973 cm^{-1} correspond to vibrational motions polarized with respect to the molecular chain, whereas the vibrational bands at 841 and 997 cm^{-1} are insensitive to the polarization conditions.¹⁶ Therefore, analysis of the intensity ratios of the vibrational bands at 809 and 841 cm^{-1} (I_{809}/I_{841}) and 973 and 997 cm^{-1} (I_{973}/I_{997}) gives information about chain orientation of the poly(propylene) molecules. Spectral line profiles and area images of the samples were composed from the measured sets of spectra using the curve-fitting tool of Grams 32 (Galactic Industries Corp., Salem, NH). The analytical Raman band used to fit spectroscopic data was the conventional product of Lorentzian and Gaussian profiles. Before the deconvolution procedure, a baseline correction was performed.

The samples were illuminated with a polarized laser, whose direction was parallel and perpendicular to

the injection direction, and the scattered radiation was collected with the same polarization conditions. The sample was placed on the stage of the Raman spectrometer with the injection direction parallel to the Z-direction of laser polarization.

Raman spectra of injected-molded PP obtained in steps of 5 μm in depth for both polarizations are shown in Figure 2. To evaluate the molecular orientation along the injection direction on the surface and volume of the test samples, the experimental values for I_{809}/I_{841} and I_{973}/I_{997} ratios versus depth are represented in Figure 3. These profiles reveal a multilayer structure with different molecular orientations. Higher orientation is exhibited for a 10- μm -thick surface layer with decreasing molecular orientation at deeper levels. The value of 1 for the intensity ratios of the X(ZZ)X polarization corresponds to a nonoriented material (isotropic) without preferential chain orientation.¹⁶ However, for an oriented sample this value is higher than 1 because the laser polarization and the

analyzer are parallel to the injection direction and most of the molecular chains have been partially oriented into this direction. It can be observed that a remanent molecular orientation inside the sample is maintained.

Depth profiles for the annealed samples at 160°C for 2 h are also presented in Figure 3. An increase in the molecular orientation in both the surface and the interior of the sample is produced. However, the variation of these values is observed continuously along the depth of the sample up to 40–50 μm from the surface. This means that the annealing process promotes molecular orientation over a larger volume of the sample.

A similar Raman analysis was performed for PP nanocomposites, to detect the influence of the clay nanolayers on the molecular orientation arising from the injection molding process. Depth profiles according to I_{809}/I_{841} and I_{973}/I_{997} ratios are presented in Figure 4. The intensity ratios show a behavior similar to that of the nonreinforced PP. Furthermore, a higher degree of chain orientation is detected on the surface, although the two-layer structure is maintained.

It can be concluded that the injection-molding process induces preferential molecular orientation along the injection direction at the surface of the PP samples, which is less pronounced inside the sample. Chain orientation is increased by thermal treatment and localized along the depth of the sample. Similar behavior was also detected in PP–clay nanocomposites, with a magnified increase in orientation for the annealed sample, mainly in a 10- μm -thick layer at the surface, suggesting the presence of residual stresses produced during the injection-molding process. Seemingly, the nanoclays act as links of the molecular chains, producing a higher chain orientation along the injection direction when the thermal treatment is accomplished.

CONCLUSIONS

Polarized confocal Raman microspectroscopy was used to analyze molecular orientation along the depth

of poly(propylene) and poly(propylene) nanocomposite-injected samples. The injection process produces preferential surface molecular orientation along the injection direction in both poly(propylene) and nanocomposite samples. The orientation is slightly increased after a thermal treatment at 160°C for 2 h, indicating the presence of residual stresses during the injection process. The final chain orientation is higher in the nanocomposite sample, especially at the surface, because the clay nanolayers act as molecular links and induce increased stress concentration.

This research was funded by the CICYT (MAT2002-04567-C02).

References

1. Motomatsu, M.; Takahashi, T.; Nie, H.-Y.; Mizutani, W. H.; Tokumoto, H. *Polymer* 1997, 38, 177.
2. Helbert, W.; Cavaill, J. Y.; Dufresne, A. *Polym Compos* 1996, 17, 604.
3. Kojima, Y.; Usuki, A.; Kawasumi, M.; Okada, A.; Fukushima, Y.; Kurauchi, T.; Kamigaito, O. *J Mater Sci* 1993, 8, 1185.
4. Oya, A.; Kurokawa, Y.; Yasuda, H. *J Mater Sci* 2000, 35, 1045.
5. Yano, K.; Usuki, A.; Okada, A.; Kurauchi, T.; Kamigaito, O. *J Polym Sci Part A: Polym Chem* 1993, 31, 2493.
6. Messersmith, P. B.; Giannelis, E. P. *J Polym Sci Part A: Polym Chem* 1995, 33, 1047.
7. Gilman, J. W. *Appl. Clay Sci.* 1999, 15, 31.
8. Gilman, J. W.; Morgan, A. B.; Harris, R.; Manias, E.; Giannelis, E. P.; Wuthenow, M. *New Adv Flame Retard Technol* 1999, 9.
9. Hilton, D.; Phillips, S. H. *Chem Mater* 2000, 12, 1866.
10. Okada, A.; Kawasumi, M.; Usuki, A.; Kojima, Y.; Kurauchi, T.; Kamigaito, O. *Mater Res Proc* 1990, 171, 45.
11. Heinemann, J.; Reichert, P.; Thomann, R.; Mulhaupt, R. *Macromol Rapid Commun* 1999, 20, 423.
12. Manias, E.; Touny, A.; Wu, L.; Lu, B.; Strawhecker, K.; Gilman, J. W.; Chung, T. C. *Polym Mater Sci Eng* 2000, 82, 282.
13. García-López, D.; Picazo, O.; Merino, J. C.; Pastor, J. M. *Eur Polym Mater* 2003, 39, 945.
14. Tabaksblat, R.; Meier, R. J.; Kip, B. J. *Appl Spectrosc* 1992, 46, 60.
15. Daman, T. C.; Porto, S. P. S.; Tell, B. *Phys Rev* 1966, 142, 570.
16. García-López, D.; Merino, J. C.; Pastor, J. M. *J Appl Polym Sci* 2003, 87, 947.